

Chaotic quantum ratchets and filters with cold atoms in optical lattices: properties of Floquet states

G. Hur, P. H. Jones and T. S. Monteiro

Department of Physics and Astronomy, University College London, Gower Street, London WC1E 6BT, U.K.

(Dated: February 9, 2020)

Recently, δ -kicked particles subjected to repeating cycles of unequally spaced kicks have been found to show quite different behavior from the Standard Map and its quantum counterpart, the Quantum Kicked Particle (QKP). In particular, experimental and calculated quantum localization lengths and ‘break-times’ are strongly dependent on the initial momentum of the particles. We investigate here the properties of the corresponding eigenstates (Floquet states) which underpin this behavior and show they differ qualitatively from those of the eigenstates of the QKP at similar kicking strengths. We use the results to analyze recent experiments with cold cesium atoms in optical lattices. For instance, we show that the ratchet effect observed in experiments [7, 9] is associated with asymmetrically localized eigenstates.

PACS numbers: 32.80.Pj, 05.45.Mt, 05.60.-k

I. INTRODUCTION

Periodically kicked quantum systems, such as the δ -kicked particle (δ -KP), which are classically chaotic, have long played a central role in studies of quantum chaos and the correspondence between quantum behavior and the underlying classical dynamics [1, 2]. An experimental realization of these systems has even been implemented with cold cesium atoms in pulsed optical lattices. This led to the direct observation of ‘Dynamical Localization’ (DL), the quantum suppression of classical chaotic diffusion [3].

Consider a usual form of the KP Hamiltonian:

$$H = \frac{p^2}{2} + K \sin x \sum_n \delta(t - nT) \quad (1.1)$$

Consider also the effect of such a Hamiltonian on an ensemble of classical particles with initially prepared with a momentum distribution, $N(p, t = 0) = \frac{1}{\sqrt{2\pi\Delta p}} \exp -[(p - p_0)^2 / (\Delta p(t = 0))^2]$, in other words a gaussian centered about some average p_0 . The classical dynamics makes a transition to chaos for a kick strength $K > \sim 1$. The ensemble diffuses in momentum space and its average energy grows linearly with time: $\langle p^2 \rangle = Dt$. The diffusion rate, to lowest order (neglecting classical correlations) is $D_0 = K^2/2$. Thus, the distribution remains a gaussian, but its width increases with time $\Delta p(t) = \sqrt{Dt}$. In contrast, the corresponding quantum system follows this behavior only up to a timescale $t^* \simeq D/\hbar^2$ [4]. For a system, whose quantum-coherence is preserved on the timescale t^* , the *quantum* momentum distribution ultimately tends to the characteristic, Dynamical Localized, exponential form: $N(p) \sim \exp -|p - p_0|/\Delta p_Q$ with constant width $\Delta p_Q \sim \sqrt{Dt^*} \sim D/\hbar$. Dynamical Localization is a wave-coherent effect: it has been verified experimentally [5] that the DL profile does not survive the presence of noise or dissipation and, with decoherence, a more gaussian profile for $N(p)$ is recovered.

In both classical and quantum cases, the behavior is independent of p_0 since, even for modest values of $K > 3$, the effects of small fluctuations in the structure of phase-space are on negligible scales relative to Δp_Q . Even if there are small stable islands, they are of size $\Delta p \sim 1$ so have little effect on the general form of $N(p)$, since typically $\Delta p_Q \gg 1$. However, it was found previously that perturbing the kick spacings T by a small amount results in large scale (relative to Δp_Q) variations in the classical momentum diffusion: these are present even in fully chaotic regimes (we take this to mean the absence of visible stable structures on the Poincare Surface of Section). For the analysis of experiments, one must then consider a local diffusion rate $D(p_0)$, in other words a diffusion rate which depends strongly on the initial relative momentum between the atoms and the optical lattice.

Two sets of unequally δ -kicked systems with local diffusion rates were previously investigated, both theoretically and experimentally [6, 7, 8]. The first is a perturbed δ -QKP (with small deviations from period-1 kicking). The second is a $2 - \delta$ KP, where the system was subjected to pairs of closely spaced kicks. These two systems were found to correspond to two distinct regimes of physical interest.

The perturbed-period system was found to yield a quantum ratchet current even in the chaotic regime (unexpected in a Hamiltonian system) [6, 9], if spatio-temporal symmetries are broken. In addition, in [6] the chaotic diffusive properties of the perturbed-period KP formed the basis for a suggestion to filter cold atoms (eg in an atom chip) according to their momenta p_0 . For the $2 - \delta$ KP, the diffusion was found to be dominated by long-ranged correlations which control escape from trapping regions in phase-space.

Both these systems localize in momentum space, but with quantum momentum distributions $N(p - p_0)$ which are not exponential and vary strongly with initial momentum p_0 . Note that the systems we consider here are always time-periodic and are quite distinct from the recent interesting study of two independent kicking

sequences, which can be non-periodic and hence non-localizing [10].

Dynamical Localization is a generic effect; it arises in an extremely wide range of different time-periodic Hamiltonians. In a time-periodic system, Floquet states perform a role equivalent to the energy-eigenstates of a conservative system, in determining the time-evolution of the initial state. Provided the underlying Floquet spectrum is made up of discrete eigenvalues (quasi-energies), the time-evolution is quasi-periodic. In the standard QKP, the Floquet states are exponentially localized; an initial state expanded in a subset of these will span only the momentum-width of these states.

In order to understand the chaotic quantum ratchet, the cold atom filter and the $2 - \delta$ KP, in this work we calculate the corresponding Floquet states and survey their localization properties. In particular, we have investigated the variation of the localization lengths, L , and the 'break-times' along with average momentum obtained from Floquet states, \bar{P} (see section III and IV). In Section II, we introduce both the perturbed δ KP and the $2 - \delta$ KP systems. In Section III, we review the calculations of the Floquet states and the localization lengths. In Section IV we present the results and in Section V, we conclude.

II. PERTURBED-PERIOD AND $2 - \delta$ KICKED SYSTEMS

The classical dynamics of the perturbed-period and $2 - \delta$ kicked systems are both given by a 2-kick map:

$$\begin{aligned} p_j &= p_{j-1} - V'(x_{j-1}) \\ x_j &= x_{j-1} + p_j T_1 \\ p_{j+1} &= p_j - V'(x_j) \\ x_{j+1} &= x_j + p_{j+1} T_2 \end{aligned}$$

For the perturbed-period KP, $T_1 = 1 - \epsilon$ and $T_2 = 1 + \epsilon$, where $\epsilon \ll 1$. Hence all we have done is to slightly perturb the kicking period about its mean. For the $2 - \delta$ KP, $T_1 = \epsilon$, $T_2 = 2 - \epsilon$. In this case we introduce a new very short time interval every second kick. Note that both systems are time-periodic, with period $T_{tot} = T_1 + T_2 = 2$.

As in the Standard Map, we consider a sinusoidal potential $K \sin x$. However, if we wish to break spatio-temporal symmetries to obtain a ratchet current, we do so by adding a 'rocking' linear potential of strength A . Hence the most general form of our potential is $V(x) = -[K \sin x + Ax(-1)^j]$, where j is the kick number. In experimental implementations of this system, the rocking linear term is obtained by means of an accelerated lattice [13].

We must consider now how the introduction of the second timescale ϵ modifies the classical behavior, relative

to the Standard Map. As stated in the introduction, for the Standard Map, if we neglect all correlations, we have a momentum diffusion rate, $D_0 \simeq K^2/2$: this is what one would expect if the atomic momenta undergo a random walk. However, unless K is exceedingly large, the Standard Map has some short-range (2-kick and 3-kick) correlations. Hence a better approximation is obtained from $D \simeq \frac{K^2}{2}[1 - 2J_2(K) - (J_1(K))^2 \dots]$. Of particular interest is the $J_2(K)K^2$ term, representing correlations $\langle V'(x_j)V'(x_{j+2}) \rangle$ between nearest-but-one kicks (the 2-kick correlation). The effects of these correlations have been experimentally measured [11].

For the perturbed-period system, it is easy to show that to lowest order the diffusion rate is unchanged. However, with correlations (for small ϵ , see [6, 7]) we have $D \simeq \frac{K^2}{2}[1 - 2J_2(K) \cos(2p_0\epsilon - A) - (J_1(K))^2 \dots]$. The key difference here is that 2-kick correlation now oscillates with the initial momentum p_0 ; this effect is most significant for values of K where $2J_2(K) \sim 1$.

The case $A = \pi/2$ is particularly interesting since then the diffusion is asymmetric about $p_0 = 0$. This implies that atoms with positive momenta will absorb energies at different rates from those with momenta of the same magnitude but moving in the opposite direction. This implies that an atomic cloud prepared initially as a gaussian centered on $p_0 = 0$ will evolve into a distribution with non-zero momentum current, $\langle p \rangle \geq 0$.

The asymmetric momentum diffusion represents a sort of chaotic ratchet (using the simple definition of a ratchet as a spatially periodic device which produces current in the absence of a net bias). This type of chaotic directed motion was first identified in a kicked asymmetric double-well potential [9] which has somewhat more complicated diffusion behavior: the ratchet mechanism (of a 2-kick asymmetric diffusion correlation) is present there too but is generally weaker (relative to the uncorrelated diffusion) and less easy to investigate since the mathematical form of the diffusion correlations is rather complex. In addition, kicked asymmetric double-well systems have not been investigated experimentally. For the above reasons we do not consider here the asymmetric double well ratchets of [9] but clearly, much of the analysis with eigenstates of the current in the system where the spatial symmetries are broken by the rocking term can be extended to the asymmetric double well.

The second system we consider in this work is the $2 - \delta$ KP. This system has diffusive behavior which is qualitatively different from the Standard Map and Perturbed-period KP. While for these other kicked systems we can analyze the diffusion as an uncorrelated term, $K^2/2$, corrected by short-ranged, typically 2 or 3-kick, correlations (for $K > 3$ or so), for the $2 - \delta$ KP, we find that the diffusion at long times is dominated by families [8] of long-ranged 'global' correlations ('global' in the sense that they correlate all kicks up to the time under consideration). At short times, the diffusion is dominated by a 1-kick correlation (not present in other kick systems); at longer times, the global diffusion terms, though weak,

accumulate and eventually become dominant.

The method of correlations provides a generic and accurate way of interpreting experimental data with cesium atoms for this system [8]. There is also a simple physical picture: for particles subjected to kicks of form $K \sin x$, consecutive kicks will be out of phase and will hence cancel if $p_0 \epsilon \simeq (2n+1)\pi$ where $n = 0, 1, 2, \dots$; in other words, an impulse $V'(x_j) = K \sin x_j$ will be immediately followed by another which cancels it, since $V'(x_{j+1}) = K \sin x_{j+1} \simeq K \sin(\pi + x_j)$. This cancellation means that particles become ‘trapped’ at these momenta. In contrast, particles for which $p_0 \epsilon \simeq 2n\pi$, will experience enhanced diffusion.

It was shown in [8] that these new types of ‘global’ families of correlations control the escape from, and through, these ‘trapping’ regions. An unexpected feature of the classical calculations (and some experimental regimes) was the observation that particles initially prepared in the trapping regions will eventually gain more energy than those initially prepared in regions of enhanced diffusion- after a timescale $t > > 1/(K\epsilon)^2$ [8].

Below we describe quantum calculations intended to improve the analysis of the experimental results for these two systems.

III. QUANTUM CALCULATIONS AND FLOQUET STATES

For δ -kicked systems, the quantum time evolution operator for one period $\hat{U}(T_{tot})$ allows a fast numerical calculation of the time-evolution of an initial wave-packet. Just like in their classical analogs, we have a ‘quantum map’ that can be iterated repeatedly:

$$\psi(t + T_{tot}) = \hat{U}(T_{tot})\psi(t) \quad (3.1)$$

There are two standard methods for implementing this quantum map. One is a split-operator technique using Fast-Fourier transforms. In the other, the time evolution operator over one period $\hat{U}(T_{tot})$ is represented as a matrix in a basis of plane waves $|l + q\rangle$ where q is a quasi-momentum and is in the range $-\pi/2 : \pi/2$. For the 2-kick systems and for a given q , the matrix elements for the evolution operator U^q , over one period, take the form [6]:

$$\begin{aligned} \langle n|U^q|l \rangle &= \exp^{-i[(T_2(l+q)^2\hbar)} \sum_j \exp^{-i(T_1(j+qa)^2\hbar} \\ &J_{l-j+ka} \left(\frac{K}{\hbar} \right) \times J_{j-n-ka} \left(\frac{K}{\hbar} \right) \end{aligned} \quad (3.2)$$

Where $ka = \text{int}(A)$ and $qa = A - ka$. Note that in this system although the one-kick operators $\hat{U}(T_1)$ or $\hat{U}(T_2)$ do not conserve quasi-momentum, the full 2-kick operator does. In consequence, as for the Standard QKP we can consider each q independently.

If a quantum state is initially expanded in the plane wave basis, (ie $\Psi_q(t=0) = \sum_l C_l q(t=0)|l+q\rangle$) it can

subsequently be evolved for each consecutive time-period by direct action of the matrix $U(T_{tot})$ on the vector of the probability amplitudes $\mathbf{C}(\mathbf{t})$:

$$\mathbf{C}(\mathbf{t} + \mathbf{T}_{tot}) = \hat{U}(T_{tot})\mathbf{C}(\mathbf{t}) \quad (3.3)$$

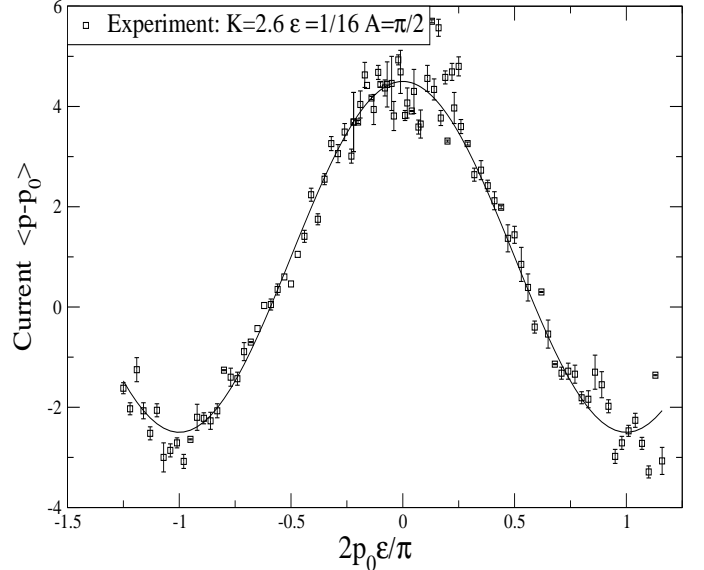


FIG. 1: Experimental values of the momentum current $I = <p - p_0>$, for the perturbed-period KP, obtained with cold cesium atoms in a pulsed optical lattice for $K \simeq 3$, $\epsilon = 1/16$. The results show that the current oscillates sinusoidally so $I \propto \cos 2p_0 \epsilon$ for $A = \pi/2$.

But as we consider the case where the Hamiltonian varies periodically with time, we can also describe the system in terms of the Floquet states Ψ_n^F (which are the eigenstates of $\hat{U}(T_{tot})$) as follows:

$$U(T_{tot})\Psi_n^F(t + T_{tot}) = \exp^{-i\varepsilon_n T_{tot}} \Psi_n^F(t) \quad (3.4)$$

where the ε_n are ‘quasi-energies’. The essence of this theory is that time-periodic Hamiltonian may be solved by methods applicable to time-independent Hamiltonians; if a quantum state $\Psi(t=0)$ is given at, $t=0$, in terms of an expansion over Floquet eigenstates, with coefficients $C_n = \langle \Psi(t=0)|\Psi_n^F(t)\rangle$, its time evolution is known at all later times from the quasi-energies ε_n :

$$\Psi(t) = \sum_n C_n \exp^{-i\varepsilon_n t} \Psi_n^F(t) \quad (3.5)$$

\hat{U} is a unitary matrix, so its eigenvalues are complex. The eigenvalues of $\hat{U}(T_{tot})$ are obtained by diagonalising the matrix form in the plane-wave basis. We employ a numerical algorithm suitable for Hermitian matrices: it can be used to obtain the spectrum of a unitary matrix U by applying it to $H^+ = \frac{1}{2}(U + U^\dagger)$ and $H^- = 1/2i(U -$

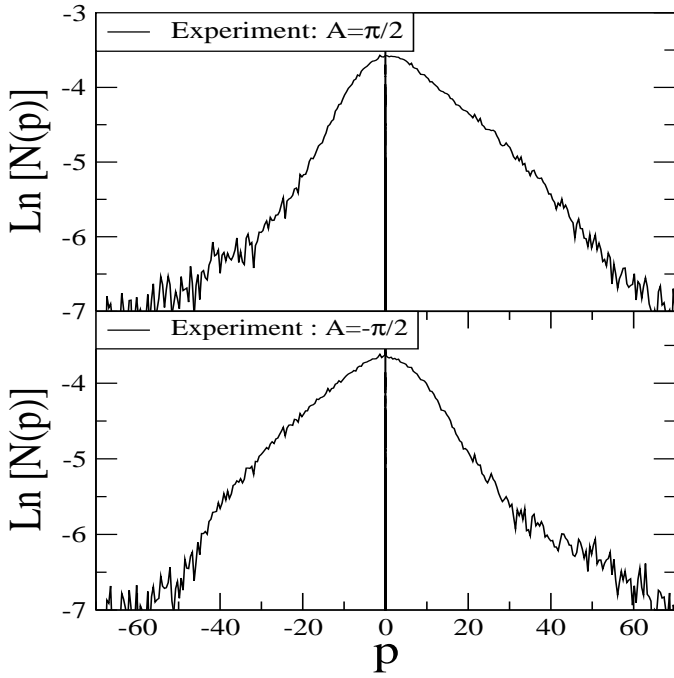


FIG. 2: Experimental momentum distributions $N(p)$ for the perturbed-period KP obtained with cold cesium atoms in a pulsed optical lattice for $K \simeq 3, \epsilon = 1/16$. The distributions have localized and hence remain essentially constant with time. The results show clearly that the origin of the net non-zero value of $\langle p \rangle$ obtained at long times is in the asymmetry of the DL profiles. As expected, the asymmetry is reversed by changing the sign of A , the amplitude of the rocking potential.

U^\dagger), where both H^+ and H^- are Hermitian. Then for an eigenvalue $e^{i\omega}$ of U , the eigenvalues of H^+ and H^- are $\cos\omega$ and $\sin\omega$, respectively [12].

Since we can make no assumptions regarding the form of $|\Psi_n^F(P)|^2$ (other than for the Standard δ -KP, the Floquet states do not generally have the simple exponential form), we represent their localization lengths by the root mean square deviation from the mean, $L_n = \sqrt{\overline{P_n^2} - \overline{P_n}^2}$ where $\overline{P_n}$ is the mean momentum of the n -th Floquet state and can be represented as $\langle n|p|n \rangle$.

IV. RESULTS: PERTURBED-PERIOD KP AND CHAOTIC RATCHET

Jones et al [13] measured a series of momentum distributions $N(p - p_0)$ as a function of p_0 for a cloud of cold cesium atoms in an optical lattice pulsed with unequal periods. Full details are given in [13], but by employing an accelerated lattice, the experiment simulated an effective rocking potential, with $A \simeq \pi/2$. The first moment of each localized distribution $\langle p - p_0 \rangle$ was then calculated and plotted as a function of p_0 . A sinusoidal oscillation $\propto \cos(2p_0\epsilon)$, with the form expected

from the 2-kick correction to the diffusion was observed and is shown in Fig.1. In particular, a distribution centered at $p_0 = 0$ initially, and with zero initial momentum current $\langle p \rangle = 0$ at $t = 0$, yielded a finite and constant momentum current $\langle p \rangle \sim 4$ at long times.

This represented the first demonstration of a fully chaotic Hamiltonian ratchet mechanism, due to the asymmetric classical diffusion. In fact, classically, a finite and persistent constant current is also obtained. It was found in [9] that asymmetric diffusion persists only on a timescale $t \sim 1/(K\epsilon)^2$ but for this unbounded chaotic system, the acquired momentum asymmetry is never lost.

For a bounded system, such asymmetries would, on a long time-scale, be averaged out since the distribution of a fully chaotic system would, then, eventually become uniform. For this reason, until recently, it was argued that a fully chaotic system could not generate directed motion. Note that, for mixed-phase space systems previously considered in [15, 16] where regions of chaotic diffusion are bounded by tori, a ratchet current generated by our asymmetric chaotic diffusive process would not persist. If there are islands, then as explained by [15], a classical ensemble initially prepared in the chaotic manifold cannot cross into the stable islands and a uniform phase-space distribution will not result. This forms the basis of the mixed-phase space ratchet proposed in [15], which represents a distinct mechanism for obtaining directed motion.

So, although as shown in [9], a fully chaotic system can keep a constant current for long times, practical implementation is less feasible since the average kinetic energy of the ensemble grows without bound. This type of chaotic ratchet is of most interest as a *quantum* rather than a *classical* ratchet since in the quantum case, Dynamical Localization halts the diffusion and 'freezes-in' the asymmetry, without the need for classical barriers like tori.

In Fig.2 we reproduce two experimental momentum distributions for $K \simeq 3$ obtained with cesium atoms by [13], for $A = \pm\pi/2$. We clearly see that the origin of the non-zero momentum current is in the asymmetric momentum distribution. The momentum distribution is essentially unchanged after about 60 kicks and the plotted values correspond to about $T = 200$ kicks.

As expected, Fig.2 shows that changing the sign of A reverses the asymmetry. At this stage it may be unclear what the significance of altering the sign of A in the experiment might be, since after all, the rocking potential involves alternating impulses $K \sin x \pm A$. In fact the distinction is between the case where an impulse $K \sin x + A$ precedes free evolution for a time interval $T_1 = 1 + \epsilon$ (obviously followed by an impulse $K \sin x - A$ and interval $T_2 = 1 - \epsilon$) and the separate experimental case where an impulse $K \sin x - A$ precedes free evolution for a time interval $T_1 = 1 + \epsilon$ and so forth (which corresponds to a reversed current).

Note that the experimental range of $K \simeq 2.6 - 3.4$ does correspond to a classical Surface of Section with some is-

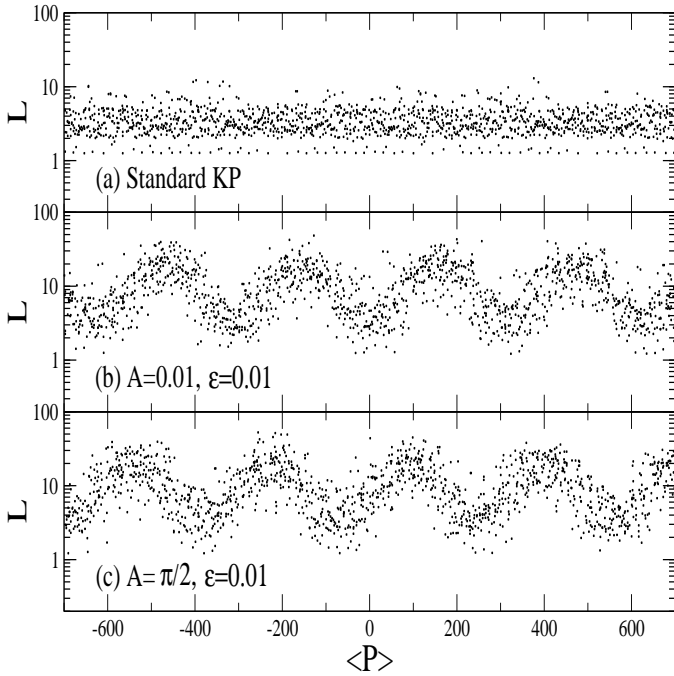


FIG. 3: The graph shows the localization lengths $L = \sqrt{\bar{P}^2 - \bar{P}^2}$ of Floquet states as a function of average momentum \bar{P} (i.e. $\langle P \rangle$) for $K=3.4$, $\hbar=1$. Results are shown (a) for the Standard KP case, i.e. $A=0.01$ (non-zero A was used to break spatial symmetry), $\epsilon=0$, (b) for $\epsilon=0.01$, $A=0.01$ and (c) $\epsilon=0.01$, $A=\pi/2$. The graph shows that for the standard kicked rotor the L are distributed within a narrow range in comparison with other two below. For the rocking case, L oscillates with \bar{P} as expected from the 2-kick correction $J_2(K) \cos(2p_0\epsilon - A)$; the oscillations of the two lower graphs are shifted relatively to each other by a phase $\pi/2$. The density of eigenstates corresponding to average momentum range is roughly the same in all three cases.

lands. However, we note that classical quantities such as the average energy are very accurately given by diffusion rates (with 2 and 3-kick corrections). The essential mechanism is asymmetric chaotic diffusion: similar behavior was found at larger K in [9] in regimes where there are no visible classical islands (but for which experiments are not available); hence, in the analysis of this type of ratchet, the presence (or otherwise) of small stable islands is immaterial. What is important though is that since the asymmetric diffusion term $2J_2(K) \cos(2p_0\epsilon - A)$, we need $J_2(K) \neq 0$. Hence the frequently studied (for the Standard Map) value $K=5$ does not produce asymmetry, since $J_2(5) \simeq 0$. Values of $K \simeq 2.5-3.5$, $\hbar=1/4-1$, on the other hand, turned out to be experimentally convenient and produced the strongest asymmetries.

We now examine the form of the underlying eigenstates. In Fig.3, we compare the localization lengths for the standard quantum KP, with those of the perturbed period KP for $K=3.4$, $\epsilon=0.01$. The difference is quite striking; while the standard QKP eigenstates are quite uniform across all regions of phase-space, the perturbed-

period localization lengths oscillate sinusoidally with \bar{P} , with a period of π/ϵ . Introducing the additional rocking potential with the accelerated lattice ($A=\pi/2$) clearly leads to a $\pi/2$ shift in the oscillations. Inspecting Fig.3(c) for $\bar{P} \simeq 0$, we see that for positive momenta the localization lengths are increasing, while for negative momenta, the localization lengths tend to a minimum. Note the nearly regular row of states for the Standard KP case with $L \simeq 1$. These correspond to states localized on a series of stable islands separated by 2π due to the momentum periodicity of phase-space in that case.

We have chosen a parameter range for which $L \ll \pi/\epsilon$: the localization length of each state is much smaller than the oscillation in \bar{P} . Hence individual Floquet states really do sample ‘local’ diffusion rates $D(p_0)$. We found that if we move towards a regime where $L \sim \pi/\epsilon$, the conclusions remain valid, but the amplitude of the oscillations is considerably damped. Similarly, if the sign of $J_2(K)$ changes, so does the sign of the sinusoidal oscillation.

We now consider the actual form of the Floquet states. In Fig.4, the momentum distributions $N(P) = |\Psi_n^F(P)|^2$ for a set of Floquet states of the standard δ -KP are shown. The distributions (with $N(P)$ on a logarithmic scale) all show the well-known ‘triangular’ form, the hallmark of Dynamical Localization. It may be clearly seen that the localization lengths vary little from state to state.

In Fig.5, in contrast, a similar plot to Fig.4, but now showing the Floquet states of the perturbed-period δ -KP, shows that the localization lengths vary strongly with the mean momentum of the state. In addition, the figure shows that for states localized close to $P=0$, there is a strong asymmetry. The states are considerably extended towards positive momentum, but are strongly localized towards negative P . This explains the form of the experimental momentum distribution of cesium atoms in the pulsed optical lattice shown in Fig.1, which for $A=\pi/2$ were also more extended towards positive P . The states localized near $P \simeq -\pi/4\epsilon$ and $\pi/4\epsilon$ correspond to, respectively, minima and maxima of the classical diffusion. They are roughly symmetrical (typically) but vary by up to a factor of $\simeq 40$ in L . In [6] it was proposed that the observed variation in the energy absorption rates between atoms prepared with an initial drift momentum $p_0 = -\pi/4\epsilon$ (which absorb very little energy) and those with $p_0 = \pi/4\epsilon$ might be exploited to ‘filter’ traffic of atoms through an optical lattice. The form of the underlying Floquet states explains this differential rate of energy absorption.

Subsequently, it was found experimentally that the $2-\delta$ KP in fact shows much more pronounced differential absorption rates. Below we report a study of the Floquet states of the $2-\delta$ -KP.

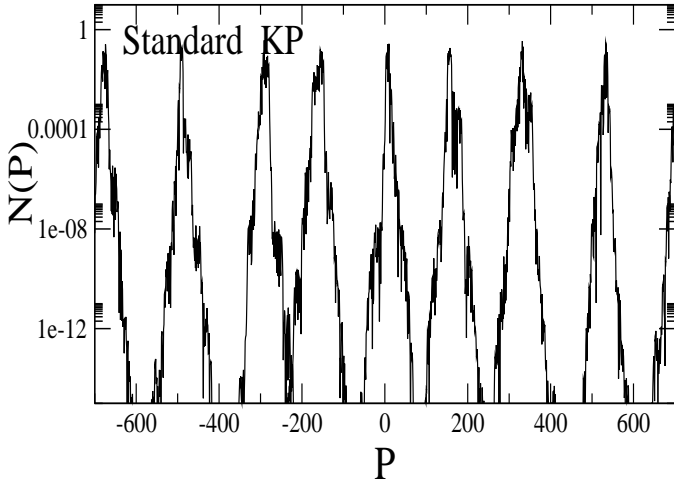


FIG. 4: Floquet states for the standard KP, for $K = 3.4$, $\hbar = 1$. As expected, all the states are exponentially localized, giving the well-known characteristic 'triangular' shape of ($N(P)$) when plotted on a logarithmic scale. They all have approximately similar localization lengths.

V. $2-\delta$ KP

A study of the experimental and classical behavior of the $2 - \delta$ KP was carried out in [8]. Here we investigate the corresponding quantum eigenstates. The classical dynamics is rather different from the perturbed-period KP. At very short times, the chaotic diffusion comprises an uncorrelated diffusion term $K^2/2$ and one dominant 1-kick correction. It was found in [8] that one can approximate the growth in the mean energy with time t , by the simple expression $\langle p^2 \rangle \simeq K^2 t [1 - \cos p_0 \epsilon]$. In Fig.6(a) experimental results for cesium atoms which localized in this regime, are shown. The experiment measured the energy of a series of clouds of $\sim 10^6$ atoms moving through the pulsed optical lattice with varying average drift momenta p_0 . For Fig.6(a), the simple expression given above gives an excellent fit to the experiment, if we take $t \sim t^*$, where t^* is the break time. This regime corresponds to $t^* \ll 1/(K\epsilon)^2$.

However, a detailed study of the classical correlations showed that for later times, a new type of correction appeared. Families of long-ranged correlations which coupled all kicks appeared. These corrections are individually very weak, but accumulate to eventually dominate the diffusive process. One family (termed the 'Poisson family' in [8]) was shown to lead to well localized inverted peaks in the energy absorption at values of $p_0 \simeq (2n + 1)\pi/\epsilon$, where $n = 0, 1, 2, \dots$. These values of p_0 correspond to trapping regions in phase-space (at low values of K , structures corresponding to islands and broken phase-space barriers are evident. However there is no need to investigate detailed transport through this complex mixed phase-space structure: the correlations give us a generic and quantitative handle of the energy diffusion with time. In this intermediate regime, dominated

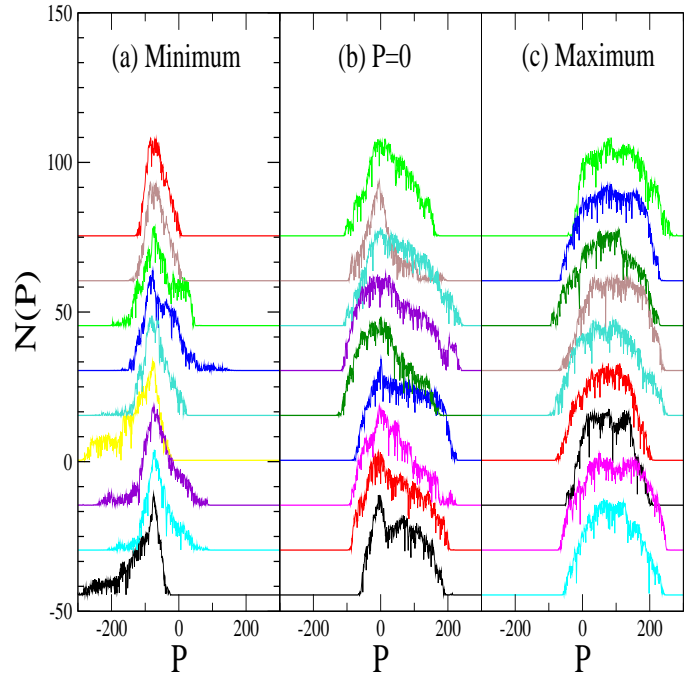


FIG. 5: Typical form of Floquet states for the perturbed-period KP, $K = 3.4$, $\epsilon = 0.01$, $A = \pi/2$ and $\hbar = 1$. Here we plot $N(P) = |\Psi_n^F(P)|^2$ as a function of P . (a) states with $P \simeq -78$. This corresponds to a minimum of the 2-kick correction $\cos 2p_0\epsilon - \pi/2$. The states are narrow, but in general, roughly symmetric. (b) states with $P \sim 0$. The typical state here is asymmetric (c) states with $P \sim +78$. This corresponds to a maximum of the 2-kick correction. States here are generally symmetrical, but broad and flat-topped.

by the 'Poisson' correlations, atoms prepared outside the trapping regions rapidly diffuse across the regions between them. Particles prepared in the trapping regions remain there. This regime occurs for $t^* \sim 1/(K\epsilon)^2$ and corresponds approximately to the experimental results shown in Fig.6.

Finally, at the longest timescales, there is the C_{G1} correction investigated in [8], which is a long-ranged 'global-correlation' family (global in the sense that it correlates all kicks, as opposed to a 1-kick or 2-kick correlation which couples only neighboring kicks). C_{G1} results in an oscillation of the form $-\cos p_0\epsilon$ and becomes dominant at the longest timescales. The oscillation is of the same period as the 1-kick correlation but is of opposite sign. This means that at the longest timescales, the minima in energy absorption shown in Fig.6(a) become maxima in energy absorption; and vice-versa: the maxima become minima. Fig.6(c) shows experiments tending towards this regime. The inverted peaks of the Poisson family are still in evidence, but a $-\cos p_0\epsilon$ is clearly superposed. This is a somewhat counter-intuitive result since it implies that atoms initially prepared in the momentum trapping regions are the ones which at long times, for $t^* \gg 1/(K\epsilon)^2$, will absorb the most energy (there are no further reversals of this behavior at even

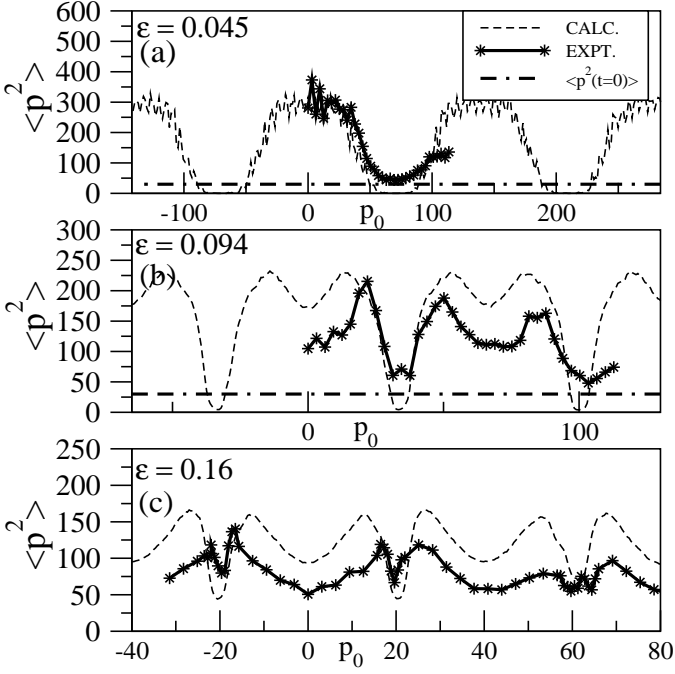


FIG. 6: Experimental results for 2δ -KP realization with cesium atoms (see [8] for details). Each data point (star) shows the energy absorbed (after 100 kicks, $K = 3.3$, $\hbar = 1$) by a cloud of atoms with average momentum $p = p_0$ (relative to the optical lattice) at initial time, $t = 0$. With increasing ϵ , we see the minima (maxima) in the energy flip into maxima (minima) as a long-ranged family of classical correlations gradually overtakes the 1-kick classical correlation. The dashed lines represent a classical simulation using 100,000 particles, all with momenta $= p_0$ at $t = 0$, and K within the range $3.3 \pm 10\%$. (a) $t^* \ll t_1 \simeq 1/(K\epsilon)^2$. Regime where a one-kick correlation is the dominant correction to the classical diffusion. Here, atoms prepared near the trapping regions ($p_0\epsilon \sim (2n+1)\pi$) remain trapped. Results follow closely the formula $\langle p^2 \rangle \simeq K^2 T / (2(1 + \cos p_0\epsilon))$. (b) $t^* \sim 1/(K\epsilon)^2$. Regime showing the inverted peaks of the Poisson correlation terms analyzed in [8], which determine the momentum trapping very close to the resonant condition ($p_0\epsilon = (2n+1)\pi$). (c) $t^* > 1/(K\epsilon)^2$. Regime dominated by correlation family C_{G1} , but sharp inverted peaks due the Poisson correlations are still visible.

longer times).

Hence, there are three distinct classical diffusive regimes, occurring at three timescales. The corresponding quantum behavior depends on which regime predominates when dynamical localization arrests the quantum momentum diffusion. In Fig.7 we show plots of $L(\bar{P})$ for the Floquet states corresponding to these three regimes.

In Fig.7(a), there is a clear sinusoidal oscillation of $L(\bar{P})$. There are additionally some extremely narrow eigenstates present for $\bar{P}\epsilon = (2n+1)\pi$. These states have widths of $L \simeq 0.01$, much narrower than states localized on stable islands (which are also visible as regular strings of points at $L \sim 1$). At the experimental values of $K \simeq 3$, for $\epsilon = 0.01$, the broadest eigenstates have

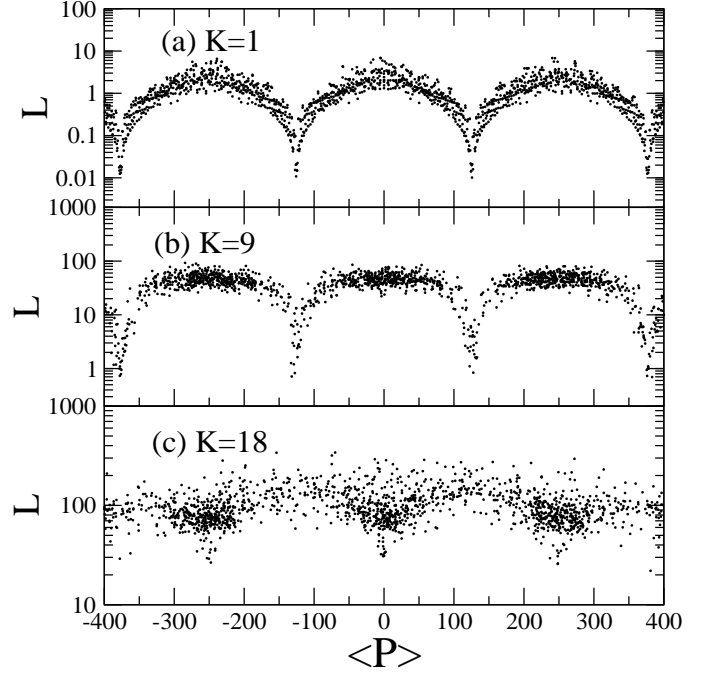


FIG. 7: Localization lengths of typical Floquet states for the 2δ -KP ($\epsilon = 0.025$) corresponding to the three classical diffusion regimes investigated in the experiments in [8].

$L \simeq 60$, while the narrowest have widths of $L \simeq 0.03$, over one thousand times narrower.

In Fig 7(b), we see a regime where, in between the momentum-trapping regions at $P \simeq (2n+1)\pi/\epsilon$, we find there is an almost constant localization length. This indicates that the eigenstates are confined between the classical broken phase barriers in the trapping regions. The typical momentum distribution here is uniform, $N(P) \sim \text{constant}$, in between the barriers and negligible outside them. Early studies indicate that the NNS level statistics are not pure Poisson in this regime as would be the case for the standard KP.

In Fig 7(c), we see a reversal of the broad cosine modulation of Fig 7(a), similar to the reversal seen in the experiment. In this regime, the eigenstates localized near $P \simeq (2n+1)\pi/\epsilon$ are typically broader than those localized in between these resonant regions.

Finally, one should discuss also the behavior of the break-times, t^* . For these systems, we also find that the break time varies strongly with momentum and follows the variations of $L(\bar{P})$. This is not unexpected: the break time is related to Δ , the mean-level spacing, of the eigenstates, i.e. $t^* = \frac{2\pi\hbar}{\Delta}$. In the experiment, our typical initial momentum distribution is a Gaussian of width $\sigma \sim 1$ (actual values are $\sigma = 3 - 6$ in the experiments reported here). If the wavepacket is prepared with drift momentum $p = p_0$, we expect that the number of Floquet states involved in the expansion in Eq.3.5 is $N \sim L(\bar{P})$ where $L(\bar{P})$ is the typical localization length for states with average momentum $\bar{P} \simeq p_0$. The quasienergies are

distributed within the interval $0 : \pi$. Therefore, we can calculate the Δ from π/N . The number of states, N , can be estimated from the states with non-negligible magnitude, $|C_n|$, of the overlap coefficients in Eq. 3.5. Hence we can also expect the same relation, $t^* \sim L(\bar{P})/\hbar$ as found with the Standard quantum case.

VI. CONCLUSION

We presented a study of the Floquet states of δ -kicked particles pulsed with unequal periods. The results were

employed to analyze experimental data on these systems. We conclude that the chaotic ratchet effect proposed in [9] and observed experimentally in [13] is associated with asymmetric Floquet states localized around $P = 0$. We conclude also that the behavior of the localization lengths of the Floquet states for the 2- δ kicked rotor broadly accompany the change over between the three distinct classical diffusion regimes investigated experimentally in [8].

- [1] G. Casati, B.V. Chirikov, Izraelev F.M., and J. Ford in “Lecture notes in Physics”, Springer, Berlin **93** , 334 (1979).
- [2] S. Fishman, D.R. Grempel, R.E. Prange, Phys. Rev. Lett. **49**, 509 (1982).
- [3] F. L. Moore, J. C. Robinson, C. F. Barucha, Bala sundaram, and M.G. Raizen Phys. Rev. Lett. **75**, 4598 (1995).
- [4] D. L. Shepelyansky Phys. Rev. Lett. **56**, 577 (1986).
- [5] B.G. Klappauf, W.H. Oskay, D.A. Steck, and M.G.Raizen, Phys. Rev. Lett. **81**, 1203 (1998).
- [6] T. Jonckheere, M. R. Isherwood and T. S. Monteiro, Phys. Rev. Lett., **91** (2003).
- [7] P. H. Jones, M. Goonasekera, H. E. Saunders-Singer and D. Meacher *quant-phys/0309149*
- [8] P. H. Jones, M. Stocklin, G. Hur, T. S. Monteiro, *physics/0405046*
- [9] T. S. Monteiro, P. A. Dando, N. A. C. Hutchings and M. R. Isherwood, Phys. Rev. Lett **89**, 194102 (2002).
- [10] J. Ringot, P. Sriftgiser, J. C. Garreau, and D. Delande Phys. Rev. Lett. **85**, 2741 (2000).
- [11] B.G. Klappauf, W.H. Oskay, D.A. Steck, and M.G.Raizen, Phys. Rev. Lett. **81**, 4044 (1998).
- [12] R. Ketzmerick, K. Kruse, T. Geisel, Physica D, **131**, 247-253 (1999).
- [13] P.H.Jones et al, to be published.
- [14] P. Reimann, Phys.Rep.**361**,57 (2002).
- [15] T. Dittrich, R. Ketzmerick, M.-F.Otto, and H. Schanz, Ann. Phys. (Leipzig) **9**,1 (2000); H. Schanz, M.-F.Otto, R. Ketzmerick T. Dittrich, Phys. Rev. Lett. **87**, 070601 (2001).
- [16] S. Flach, O. Yevtushenko, Y. Zolotaryuk, Phys. Rev. Lett. **84**, 2358 (2000).